

Examining high-resolution survey methods for monitoring cliff erosion at an operational scale

Letortu Pauline ^{1,*}, Jaud Marion ², Grandjean Philippe ³, Ammann Jerome ², Costa Stephane ⁴,
Maquaire Olivier ⁴, Davidson Robert ⁴, Le Dantec Nicolas ^{2,5}, Delacourt Christophe ²

¹ Univ Bretagne Occidentale, CNRS, UMR LETG, IUEM, Rue Dumont Urville, Plouzane, France.

² Univ Bretagne Occidentale, CNRS, UMR Geosci Ocean, IUEM, Rue Dumont Urville, Plouzane, France.

³ Univ Lyon 1, CNRS, UMR Sci Terre, 2 Rue Raphael Dubois, Batiment GEODE, Villeurbanne, France.

⁴ Normandie Univ, UNICAEN, CNRS, UMR LETG, Esplanade Paix, Caen, France.

⁵ Direct Eau Mer & Fleuves, CEREMA Cerema, 134 Rue Beauvais, Margny Les Compiègne, France.

* Corresponding author : Pauline Letortu, email address : pauline.letortu@univ-brest.fr

Abstract :

This paper aims to compare models from terrestrial laser scanning (TLS), terrestrial photogrammetry (TP), and unmanned aerial vehicle photogrammetry (UAVP) surveys to evaluate their potential in cliff erosion monitoring. TLS has commonly been used to monitor cliff-face erosion (monitoring since 2010 in Normandy) because it guarantees results of high precision. Due to some uncertainties and limitations of TLS, TP and UAVP can be seen as alternative methods. First, the texture quality of the photogrammetry models is better than that of TLS which could be useful for analysis and interpretation. Second, a comparison between the TLS model and UAV or TP models shows that the mean error value is mainly from 0.013 to 0.03m, which meets the precision requirements for monitoring cliff erosion by rock falls and debris falls. However, TP is more sensitive to roughness than UAVP, which increases the data standard deviation. Thus, UAVP appears to be more reliable in our study and provides a larger spatial coverage, enabling a larger cliff-face section to be monitored with a regular resolution. Nevertheless, the method remains dependent on the weather conditions and the number of operators is not reduced. Third, even though UAVP has more advantages than TP, the methods could be interchangeable when no pilot is available, when weather conditions are bad or when high reactivity is needed.

Keywords : Coastal cliff erosion, monitoring, terrestrial laser scanning, terrestrial photogrammetry, UAV photogrammetry, Normandy

40 **1 Introduction**

41 Changes to coastal cliffs are complex because of the sudden and stochastic natures of
42 erosion in time and place and the diversity of movements (rock falls and debris falls
43 according to the typology of Varnes). Despite contributions to research into
44 geomorphological processes on rocky coasts in recent years, the respective contribution
45 of the triggering factors responsible for erosion is still difficult to determine (Naylor et
46 al. 2010; Lim et al. 2011; Letortu et al. 2015a; Laute et al. 2017).

As quantifying changes in unstable and subvertical cliff face is difficult and sometimes dangerous, in situ data are mainly collected by remote-sensing methods. Data with a horizontal or quasi-horizontal point of view (side scanning a vertical structure as the cliff face) allow all changes to be observed because the data capture cliff face changes which reflect failures and deposits anywhere on the cliff profile (contrary to cliff top and cliff base). High spatial resolution and high temporal repetitiveness are essential to reveal patterns of cliff failure (location, time) and therefore to better understand and forecast the processes responsible for cliff erosion (e.g. Collins and Sitar 2008; Hampton 2002; Vann Jones et al. 2015; Young 2015).

Different methods terrestrial Laser Scanning (TLS), Aerial Laser Scanning (ALS), Mobile Laser Scanning, Unmanned Aerial Vehicle Photogrammetry (UAVP), Terrestrial Photogrammetry (TP) are available for cliff monitoring depending on the precision, the spatial and temporal scales, and costs (e.g., Young et al. 2010; James and Robson 2012; Michoud et al. 2014). As reported in James and Robson (2012), for restricted areas (ranges of 10–500s of meters) terrestrial laser scanners or TP can be used. Over larger areas, aerial photogrammetry, aerial laser scanners, and space-based radar and photogrammetric techniques are possible.

Within the framework of the “Service National d’Observation DYNALIT” (French National Service Observation for the study of coastal and coastline dynamics), we survey the cliff-face evolution in Petit Ailly site in Varengeville-sur-Mer (Normandy, France) to quantify fine-scale changes, to visualize the modalities of evolution and to contribute to the debate about the agents responsible for the retreat of the chalk cliffs. Since October 2010, a 3D monitoring of the cliff face has been performed by terrestrial laser scanner (an active remote-sensing instrument) at very high spatial resolution and with pluricentimeter precision (± 0.03 m) every 3–4 months

(Letortu et al. 2015b). It enables reliable, homogeneous, frequent and perennial monitoring of rock falls and debris falls. However, the TLS routine is expensive and cumbersome and therefore requires several operators. UAVP and TP surveys may be efficient alternatives offering data of equivalent quality.

Is the accuracy of close-range techniques, such as TP and UAVP, sufficient in comparison with the more expensive and cumbersome TLS routine for monitoring cliff-face erosion? The answer to this question involves many topics: (1) the resolution and/or ground sampling distance (2) the spatial coverage (3) the accuracy and precision of the datasets for diachronic surveys of individual and mass movements, and (4) an easy-to-use acquisition protocol for the site configuration and data processing. If the different techniques achieve the same level of data quality, these methods could be interchangeable, depending on weather conditions and people availability, without any impact on the monitoring results.

Thus, this article presents an original comparison for such environment of three high-resolution remote-sensing methods implemented for 28 January 2016: (1) measurement by TLS and two photogrammetric methods based on Structure from Motion/Multi-View Stereophotogrammetry (SfM-MVS) techniques from (2) UAV photographs and (3) terrestrial photographs. After a brief description of the study area, this paper details the survey methodology. Finally, the results of the cliff-face monitoring are presented and discussed.

2 Study area

The study takes place near Dieppe, in Seine-Maritime (Normandy) in the northwestern part of France and along the Channel. Geologically, the Upper Normandy coastal cliffs (60-70 m high on average) extending from Cap d'Antifer to Le Tréport (100 km) are

made of various chalk with flints of Upper Cretaceous (Pomerol et al. 1987; Mortimore and Duperret 2004). The different stages of chalk (from the oldest to the newest: Cenomanian, Turonian, Coniacian, Santonian and Campanian) present slight variations in facies and fine sedimentary discontinuities, inducing some subtle resistance contrasts. Over these chalk strata, the usual residual flint formation (Laignel 1997; Costa et al. 2006) have been replaced by a bed of clay and sand sediments about 10-30 m thick of Paleogene age (Bignot 1962), especially in Sainte-Marguerite-sur-Mer, Varengeville-sur-Mer, and Sotteville-sur-Mer (Figure 1). The Seine-Maritime cliff coast is characterized by the regressive dynamics, coming out as instantaneous falls affecting all or part of the cliff. A monitoring of the regressive dynamics of the cliff top between 1966 and 2008 shows a retreat rate of 0.15 m/year with high spatial variability in Upper Normandy (Letortu et al. 2014).

The SNO DYNALIT site of Petit Ailly is located along Cap d'Ailly (<https://www.dynalit.fr/fr/falaises/ailly-puys>). More precisely, it lies on either side of the Petit Ailly dry valley in Varengeville-sur-Mer (Figure 2). This site is made up of Santonian chalk, covered by a bed of clay and sand of Paleogene age, prone to erosion. It has a high erosion rates calculated from TLS surveys: from October 2010 to June 2017, the erosion rate is 0.38 m/year with a fallen volume of 12965 m³ (± 155 m³) due to rock falls and debris falls. Nevertheless, these average retreat rates are not representative of the erosion which occurs suddenly caused by rockfalls. For example, in February 2014, a rock fall of approximately 5000 m³ resulted in a cliff-top retreat of 11 m in a few seconds.

The studied cliff face is characterized by (1) its verticality (from 70° to overhang); (2) its height (about 30-40 m); (3) its spatial extent (250 m long); (4) debris falls, which are individual movements of blocks or flakes (up to decimeters), and rock

falls, which describe large-scale mass movements from all or part of the cliff face; and
(5) its limited accessibility (rock falls, tide constraints, difficulty in setting up targets at the cliff top).

3 Methods

3.1 Data collection

3.1.1 Terrestrial laser scanner data collection and ground control points

A terrestrial laser scanner is an optical active remote-sensing technology that can measure the position (distance and angle) of a point relative to the device using the time of flight of laser pulses reflected by the point to be measured.

The instrument used in this study is a Riegl® VZ-400 (Figure 2(6)) emitting a laser pulse in the near-infrared (1550 nm), which records unique echo digitization but allows the digitized echo-signals (waveform data) to be processed in Riegl® software. This instrument provides scan data acquisition with theoretical 0.005 m accuracy and 0.003 m precision at a range of 100 m. The measurement range can reach up to 600 m while the measurement rate can reach up to 122,000 measurements per second with a wide field of view of 100° vertical (from 30° to 130°) and 360° horizontal (Riegl 2014). Moreover, the Riegl® VZ-400 is equipped with a Nikon D800 camera, which provides photographs. These pictures can be used to drape a 2D image on the 3D point cloud but are not an absolute requirement for topographic measurement. In Varengeville-sur-Mer, the two scanner stations are positioned on the beach at about 75 m from the cliff face. TLS acquisition involves a 360° horizontal and 100° vertical scan with an angular resolution of 0.04° in both directions, providing a dense 3D point cloud (more than 22.5 million points) and five photographs in 9 min (20 % overlap by default). These

instruments are heavy, 20 kg for the scanner and 1 kg for the Nikon camera, and require complementary equipment (a tripod, cases, batteries, targets and a total station).

To carry out georeferencing and obtain repeated surveys of high accuracy, the data acquisition process requires additional equipment: reflective targets (10cm high cylinders, 0.15 kg, Figure 2(4)) used as ground control points (GCPs) and a total station to measure them (Figure 2(2)). Contrary to the GPS, the total station measures points close to the cliff front without a mask effect. The Trimble M3 total station is precisely positioned at a single location previously known by raw data GPS post-processing. Knowing the reflective targets absolute coordinates enables the point cloud acquired in a relative coordinate system to be projected in an absolute coordinate system (Lambert 93 and associated RGF93 and IGN69, official reference system in France; EPSG: 2154). For the TLS survey at Petit Ailly, laser scans were performed from two stations with 15 targets as GCPs (Figure 3). To reduce the alignment error of the point cloud, targets are numerous and with different distances from the scanner (as long as they all remain visible).

3.1.2 Terrestrial photo collection

Terrestrial photographs are acquired with a Nikon D800 reflex camera (1 kg) with a focal length of 35 mm, taking 36 Mpix photos. To collect data on the cliff front, as recommended by James and Robson (2012), images of the area of interest are acquired from different positions. As depicted in Figure 5a, the camera orientations are not parallel but rather converge on the scene. The procedure to collect digital photographs is quite easy to implement. It involves short distances between the acquisition positions (around 2–3 m when taking photos at ~20 m from the cliff foot) and photos taken at angular intervals of 10–20°, over a wide range of angles. To obtain a high-quality

dataset, photographs should overlap by at least 60 % (ideally, a point should be seen at least three times) and must capture the area with at least two shooting angles. In 23 min, the whole cliff section (250 m long) was covered by a dataset of 153 photographs collected along the baseline depicted in Figure 3. The overlap enables that any point in the studied cliff face being present in six to more than nine photographs.

3.1.3 UAV photo collection

The drone survey is implemented using an electric hexacopter UAV, called DRELIO 10 (multi-rotor DS6 platform assembled by DroneSys). A collapsible frame enables it to be folded for easy transportation. With a 0.8m diameter, the DRELIO 10 weighs less than 4 kg and can handle a payload of 1.6 kg. The flying time is about 20 min. On a tilting gyro-stabilized platform, a Nikon D800 reflex camera with a focal length of 35 mm is set up. The camera takes 36 Mpix photographs in intervalometer mode every 2 s. The DJI[®] software iOSD runs the flight control. For delicate steps of the take-off and landing, the pilot prefers to control the UAV thanks to ground station software.

The dataset is collected along the yellow baseline depicted in Figure 3. As shown in Figure 5b, data at the cliff top were collected by the camera that is in the nadir position. To collect data on the cliff front, the camera was forward-pointed and tilted at 25°. In this case, the flight has to be performed in manual mode to keep the camera turned toward the cliff face. The flight lasted around 8 min. In this configuration, the dataset is composed of 110 oblique and nadir images (that will be processed together), any point in the studied cliff face being present at least in 9 photographs.

3.1.4 GCPs for TP and UAVP

Like the TLS survey, TP and UAVP need GCPs (targets) to record the models in a reference coordinate system and to achieve models of the highest quality, in terms of

both geometrical precision and georeferencing accuracy. The absolute coordinates are provided by additional equipment : the total station (previously described). In order to obtain a high-quality final model (James and Robson 2012) and help to mitigate doming effects caused by an incorrect camera model and radial distortion (James and Robson 2014), a large number of GCPs is recommended. The GCPs need to be distributed throughout the area of interest (Javernick et al. 2014; Smith et al. 2014) without linear configurations. They should ideally cover both the margins and the center of the area of interest, with a good range of values in each spatial dimension. However, in a cliff context, access to the cliff face is dangerous due to frequent rock falls. It can therefore be difficult to ensure targets are clearly visible while guaranteeing the safety of the person installing them at the top of the cliff. The lack of targets on the upper part of the cliff face may create distortion. To avoid this concern, the photograph acquisition protocol was implemented cautiously. The UAV camera was forward-pointed and tilted at 25° with photographs at different distances from the cliff face to reduce distortion. For TP, a great variety of viewing angles of terrestrial photographs was taken to limit the doming effect (Jaud et al. 2017b). A total of 17 targets were used for TP with different configurations: 9 were vertically positioned on the area of interest (center of orange crosses, 40 cm high, painted on the lower part of the cliff face, Figure 2(5)) while 8 targets (circular disks, 23 cm in diameter, Figure 2.1) were horizontally positioned on the beach (Figure 3). For UAVP, 22 targets (circular disks, 23 cm in diameter, Figure 2(1)) were horizontally positioned on the beach, on the lower part of the valley slope and on the cliff top (Figure 3).

3.2 Data processing

3.2.1 Terrestrial laser data processing and absolute error quantification

The main steps in the TLS data processing are (1) georeferencing and point cloud assembly (RiscanPRO® software); (2) manual point cloud filtering including areas without overlap with previous TLS data, noise and vegetation (Fledermaus®); and (3) Delaunay 2.5D meshing (best fit plane, Cloudcompare®).

The scanning survey of each position is recorded as a 3D point cloud (x,y,z) in a reference system relative to each position of the scanner in the field. The accuracy of georeferencing is carried out by comparing the position of the control points in the model with the GCPs precisely measured on the field using the Root Mean Square Error method (measuring the differences between values predicted by a model and the values really observed) (Kaiser et al. 2014; Eltner et al. 2016). This accuracy assessment is only valid if the point cloud is considered consistent (distortion due to atmospheric effects is neglected). For the first and second stations, the standard deviations of fit residues are 0.0091 and 0.0093 m, respectively. The absolute error on the data (accuracy) is the sum of the TLS instrumental errors, the total station measurement errors, and topographic inaccuracies during georeferencing. The theoretical instrument accuracy of the TLS is very high (± 0.005 m at a range of 100 m), so the main source of error comes from the total station survey, which measures the target positions with accuracy from 0.01 to 0.03 m.

In a context of recurrent TLS surveys, a procedure of accuracy assessment has been implemented. It is based on the comparison of the position of 3 fixed points (surveyor nails located on the descending road to the sea) measured by the total station during the 18 successive missions carried out within the framework of the DYNALIT observatory. The 6 July 2011 topographical survey is defined as a reference because the

survey conditions were optimal. Identified thanks to their dispersion from the reference data, the poor measurements are removed. The validated data have a maximum dispersion ellipse of 0.018 m in x, 0.019 m in y and 0.033 m in z (Figure 4).

For diachronic comparisons to quantify local erosion rates, the point clouds are adjusted relative to this point cloud of reference (6 July 2011) using a best fit algorithm. To keep the consistency of this protocol, the comparison between TLS data and photogrammetric data is also based on a best fit adjustment.

3.2.2 Photograph data processing and precision

The procedure for deriving 3D point clouds from photographs is based on the SfM-MVS workflow. The SfM-MVS algorithm is implemented by AgiSoft® PhotoScan Professional (version 1.2) (Figure 5). The positions of the GCPs are imported into Agisoft® PhotoScan and, concurrently, the GCPs are pointed out on the photographs to compute the georeferenced 3D point cloud.

The 3D surface reconstruction is divided into two main steps:

- Camera alignment by bundle adjustment. Tie points are detected and matched on overlapping photographs so as to compute the external camera parameters (position and orientation) for each picture. From 17 to 22 GCPs (targets located on the cliff front and on the beach for TP; targets on the beach for UAVP) are tagged to georeference data and refine the internal parameters of the camera.
- From the estimated camera positions and the pictures themselves, stereophotogrammetric equations allow the software to compute the position of each tie point, so as to build a dense point cloud.

There is no direct measurement of accuracy from TP or UAVP because the surveyor nails (fixed in a horizontal position) are not always visible in these datasets. TLS data are considered the reference dataset for comparison in this paper, so, as previously mentioned, TP and UAVP point clouds have been fitted to TLS data. Therefore, the measure of precision of the photogrammetric reconstruction for TP and UAVP datasets is assessed relative to the synchronous TLS dataset. The best fit RMS error is of 0.04 m between TP and TLS and UAVP and TLS.

3.3 Data comparison

First of all, TLS and photogrammetric methods (UAVP and TP) differ in the nature of collected data and so resulting products. The main advantage of UAVP and TP is that they provide textured models of better quality than the TLS model. When scanning a site, by default, the TLS takes only five photographs for a 360° horizontal angle (with an overlap of 20%). This is not enough to create, from all angles, a textured model taking into account the terrain (Figure 6b). It is possible to increase the overlap but because of fixed points of view of TLS stations, it would be hard to match the photogrammetric model. In fact, the process of SfM-MVS itself involves the use of ten(s) of high-resolution photographs, thus enabling the algorithm to choose perfectly the relevant photographs to texture each parcel of the model (Medjkane et al. accepted). It thus constitutes an important asset for the morphological analysis and interpretation of landscapes (Figure 6c and d).

A first comparison of raw data is provided in Table 1. For the TP dataset, because the photographs were taken closer to the cliff face than for the other datasets, more photographs were needed to cover the area of interest so the sampling distance on the cliff face was greater than for UAVP (Table 1). The volume of data was so large

that it was not manageable; it had to be processed in chunks. The steps for a more advanced quantitative comparison were

- (1) Cleaning the point cloud around the cliff face to obtain a good surface overlap;
- (2) Subsampling TP and UAVP datasets to obtain manageable ones. The distance sampling was a point every 0.06 m to have the same mean sampling as the TLS point cloud, considered the reference;
- (3) Fitting TP or UAVP models to the TLS point cloud used as the reference with Cloudcompare and 3DReshaper software; and
- (4) Comparison of the subsampled fitted point clouds (TP_SF, UAVP_SF) with the TLS mesh (2.5D Delaunay mesh).

After dataset subsampling (0.06 m) of TP and UAVP models, quick filtering around the cliff face and the beach and a fitting between TP or UAVP models and the reference data (i.e. the TLS point cloud), the final point clouds can be quantitatively compared (Table 2).

As in many papers (Westoby et al. 2012; Kaiser et al. 2014; Eltner et al. 2015; Smith et al. 2016), we consider TLS models as the reference although they may also have bias. As declared by Kromer et al. (2015), “the ability to detect change by comparing a series of point clouds is controlled by the point cloud accuracy, precision, survey design and terrain factors.” For the TLS point cloud, these parameters are, as Kromer et al. (2015) point out:

the scanner target distance (Teza et al. 2007), vegetation (Su and Bork 2006), incidence angle (Sturzenegger and Stead 2009; Lato et al. 2010; Pesci et al. 2011), surface reflectance (Csanyi and Toth 2007), surface roughness (Lague et al. 2013), atmospheric conditions (Beckmann 1965), heterogeneity in point spacing (Raber et al. 2007), alignment error (Oppikofer et al. 2009) and instrument specifications (Pirotti 2013). Some of these factors contribute to the random Gaussian point-to-

point noise (precision), and others contribute to a systematic error (Lichti and Skaroud 2010).

However, we consider the TLS dataset the reference in this relative comparison because (1) within the TLS dataset, measurement errors related to the accuracy of the laser are constant (0.005 m at a range of 100 m) while errors inherent in georeferencing are transmitted to the whole cloud; (2) vegetation is scarce on the cliff face; (3) the incidence angle is close to the normal direction and so the noise and systematic error of the TLS point cloud are likely to be low.

For a quantitative data comparison, four calculation algorithms can be used (Kromer et al. 2015): (1) M3C2 (2) mesh to point or mesh to mesh change detection (3) spatial filtering (with calibration) and (4) space-time filter (with calibration). We used mesh (for the TLS dataset) to point (photogrammetry datasets) because (1) the spatial distribution of density from TLS, TP, and UAVP is different leading to an overassessment of the distance between points; (2) the shortest distance calculation enables change in different directions to be interpreted; and (3) noise is reduced through the creation of the mesh of TLS data.

4 Results and discussion

4.1 Global quality assessment

The characteristics of the resulting point clouds differ from one method to another (Table 2). As shown in Figure 7:

- The spatial distribution of the density is highly variable within the TLS point cloud due to the positions of the TLS stations. The most homogeneous densities are unsurprisingly UAVP and TP not only because of subsampling but also

because of the *modus operandi*, with a moving point of view during data collection. UAVP has the most homogeneous density due to the automatic snapping every 2 s.

- The best spatial coverage is observed for the UAVP model with no occlusion.

With the subsampled fitted (SF) point clouds, the comparisons of TP_SF and UAVP_SF datasets with the TLS dataset highlight the low error value (millimeter to centimeter values), which is relevant to observe debris falls. The mean error value is mainly from 0.013 m to 0.03 m (Figure 8c and d). However, artifacts on datasets have values superior to 1 m. These artifacts could be partially due to the error-assessment method overestimating the error when the point cloud density is drastically different between the compared datasets (because of occlusion).

Over the whole datasets, the mean error value is of 0.005 m for the TP model, whereas it is of 0.014 m for the UAVP one. Thus, the TP model is more precise than the UAVP one relative to the TLS reference. Nevertheless, the standard deviation is lower for the UAVP_SF model than for the TP_SF one, so the dispersion of the measurement error is lower (Table 3). In our comparison, the most important issue is to have a low measurement error dispersion in order to obtain a reliable dataset (Figure 8a and b), and so, for this purpose, the UAVP dataset appears to be the most relevant.

During data acquisition, the three datasets may suffer from occlusion due to terrain factors (rock falls, overhanging areas, hollow areas, vegetation, and caves). Occlusion is minimized with the TP and UAVP surveys relative to the TLS surveys because the SfM-MVS survey covered the whole cliff face thanks to a greater number of points of view. The UAV flight provides the largest number of cliff-face views and can avoid the concern about overhanging. With the TLS surveys, time limitations determine the number of possible tripod set-ups meaning that gaps may occur in the

final point cloud owing to occlusion. In such a context, a small number of targets are an important issue because decreasing the duration per station will improve the spatial coverage and the accuracy of the TLS surveys (Jaud et al. 2017a).

4.2 Local quality assessment

In the previous data comparison, when a point in one dataset is situated in a zone without data (due to occlusion) in the compared dataset, the point to mesh distance is measured relative to the nearest point, introducing an overestimation of the error. To avoid this, we defined strips of the cliff face (Figure 9) considered to be without artifacts in the error assessment (without vegetation, rock falls, complex morphology, occlusion, etc.).

First, for all cliff-face strips, both data comparisons give nearly the same mean error (0.015 m for TP-TLS comparison and 0.016 m for UAVP-TLS comparison) and standard deviation values (0.031 and 0.026 m, respectively, for TP-TLS and UAVP-TLS comparisons). So, without occlusion, the results from both methods seem to be comparable.

Second, the mean error values are similar between the whole cliff face and strips for UAVP (0.014 and 0.015 m, respectively). The standard deviation is slightly lower for the strips than for the whole cliff face (0.026 against 0.037 m) due to surface homogeneity, which limits overestimation. For TP, the results are different. The mean error value is higher for the strips than for the whole cliff face (0.016 and 0.005 m, respectively), whereas the standard deviation is lower for the strips than for the whole cliff face (0.031 and 0.05 m, respectively). This means that occlusion significantly affects the TP results. UAVP appears to be a more reliable and stable method whichever

surface is studied (cliff-face morphology, vegetation, etc.) whereas TP is much more sensitive to roughness.

4.3 Elements for choosing a relevant survey method

According to our results, the choice of a suitable method for cliff erosion monitoring depends on many criteria that are summarized in Table 4.

The main advantages of TLS are the precision of the data and the low dispersion due to the consistency of the dataset (including the georeferencing step). Another advantage is the long battery life, which enables many surveys to be carried out, especially if the distance between stations can be increased to cover a larger area and a single target can be used per survey (visible from every TLS station). The main disadvantages of TLS remain the very expensive purchase and maintenance costs and the weight. TLS field campaigns have low ability to implement survey because the stations have to be close to the area of interest and the instrument is heavy (50 kg including instruments, cases, batteries, a tripod and targets) and cumbersome. Easy access to the area is necessary. Moreover, the weather conditions are a restraining factor (in addition to tide times) since the instrument is highly sensitive to rain, wind, and fog, which may be frequent in coastal areas (Table 4). The alternative of a hand-held mobile laser scanner, which has been recently used for cliff-erosion monitoring (James and Quinton 2014), could overcome the portability concern but the purchase of new material is not desirable.

The main strengths of TP are very long battery life, very low sensitivity to bad weather, very good ability to implement survey, and low cost. Because this method needs a light instrument, which has a low energy consumption, the survey can be done with the highest battery life. Thanks to these major advantages, the survey can be highly

reactive and easily carried out before/during/after a morphogenesis event. The main weaknesses are the dispersion of the data and the processing duration (Table 4).

The main strengths of UAVP are the *modus operandi*, which can be adapted to the configuration of the study area (very high flexibility in the ability to capture the interest area) and very high speed of data acquisition. With a UAV pilot, sites that are difficult to access can be monitored since the take-off and landing can be in the hinterland. With a suitable flight plan, the distance-to-target can be varied to avoid occlusion due to topographic complexities (Abellan et al. 2016). However, having a pilot available (a key skill) can be a major constraint and weather conditions have to be dry, with neither strong wind nor fog. Mild weather conditions may be a limiting factor in coastal zones. Moreover, as TP, the duration of data processing may be longer than for the TLS data (Table 4).

In the context of the observatories, the camera network (photo or video) could be a complementary approach. More precisely, this instrumentation would not be used for a precise quantification of observed changes but seems more suitable for a site of a hundred meters maximum to capture erosion events because of its higher temporal resolution. In fact, the time sampling of the TLS, PT, and UAVP surveys does not provide this kind of information. The precise time of the observed change is important to constrain the driving forces and, if possible, identify the triggering factor. Moreover, with this information, a quantification survey can be planned when necessary. Thus, video monitoring, combined with the precise quantification of changes thanks to TLS, UAVP or TP, could improve the understanding of the agents and processes responsible for cliff erosion and failure forecast. However, deployments of video cameras are not possible everywhere because of the site configuration. A camera network needs to be

installed on a fixed support (e.g., on large rocks that can protect cameras from waves, spray and abrasion) with a suitable view angle (embayed coast). Each of the techniques presented in this paper has different strengths and weaknesses. The choice of the instrument(s) (it could be a combination) to carry out monitoring depends on the required precision, the costs, the site configuration (accessibility, height, danger, morphology, etc.), the time, the people and skills available, as well as the weather conditions and legal framework (for UAV).

5 Conclusion

Because the precision of a centimeter range (mean error value from 0.013 to 0.03 m) is reached by the TP and UAVP, these can be seen as complementary methods to TLS cliff erosion monitoring in Normandy. However, it should be remembered that TP is sensitive to roughness, which can increase the standard deviation of data. Moreover, in order to obtain textured models of good quality, SfM-MVS models are clearly better than those of TLS. Because the TLS survey is cumbersome and expensive, the lower costs of TP or UAVP seem attractive. However, it is important to bear in mind that the choice is specific to accuracy expectations; the site configuration (accessibility, height, danger, morphology, etc.); the time available to do the survey; the people and skills available; financial resources; weather conditions and the legal framework (for UAV). For our cliff erosion survey, TLS remains a good option because the methodological framework can be improved (e.g. a single target) but UAVP is an interesting alternative: (1) with a large spatial coverage in a few minutes with numerous viewpoints that avoid occlusion; (2) a lighter weight and a higher flexibility in the ability to capture interest areas than TLS; and (3) easy site access because the take-off and landing can occur in the hinterland. However, this method needs a qualified pilot and if the area of interest is

near sensitive stakes (houses, airports, etc.), it could take time to obtain the flight authorization. Another main weakness is its high sensitivity to weather conditions (especially wind and rainfall), which can delay many surveys in the coastal zone. Therefore, if a reactive method is needed, TP could be a good option. Despite some drawbacks, SfM-MVS has changed topographic data collection in a wide range of environmental settings and should have a bright future because of technical developments in the devices and software.

References

- Abellan, A., Derron, M. H., and M. Jaboyedoff. 2016. "Use of 3D Point Clouds in Geohazards. Special Issue: Current Challenges and Future Trends." *Remote Sensing* 8 (130). doi:10.3390/rs8020130.
- Beckmann, P. 1965. "Signal degeneration in laser beams propagated through a turbulent atmosphere." *Journal of Research of National Bureau Standards. Sect. D: Radio Science* 69D: 629-640.
- Bignot, G. 1962. "Étude sédimentologique et micropaléontologique de l'Éocène du Cap d'Ailly (près de Dieppe, Seine-Maritime)." PhD diss., University of Paris.
- Collins, B. D., and N. Sitar. 2008. "Processes of coastal bluff erosion in weakly lithified sands, Pacifica, California, USA." *Geomorphology* 97: 483-501.
- Costa, S., Laignel, B., Hauchard, E., and D. Delahaye. 2006. "Facteurs de répartition des entonnoirs de dissolution dans les craies du littoral du Nord-Ouest du Bassin de Paris." *Zeitschrift für Geomorphologie* 50: 95-116.
- Csanyi, N., and C. K. Toth. 2007. "Improvement of lidar data accuracy using lidar-specific ground targets." *Photogrammetric Engineering & Remote Sensing* 73: 385-396.
- Eltner, A., Baumgart, P., Maas, H. G., and D. Faust. 2015. "Multi-temporal UAV data for automatic measurement of rill and interrill erosion on loess soil." *Earth Surface Processes and Landforms* 40: 741-755.
- Eltner, A., Schneider, D., and H. G. Maas. 2016. "Image-based surface reconstruction in geomorphometry - merits, limits and developments." *Earth Surface Dynamics* 4: 359-389.

485 Hampton, M. 2002. "Gravitational failure of sea cliffs in weakly lithified sediment."
 486 *Environmental and Engineering Geoscience* 8 (3): 175-191.

487 James, M. R., and J. N. Quinton. 2014. "Ultra-rapid topographic surveying for complex
 488 environments: the hand-held mobile laser scanner (HMLS)." *Earth Surface*
 489 *Processes and Landforms* 39: 138-142.

490 James, M. R., and S. Robson. 2012. "Straightforward reconstruction of 3D surfaces and
 491 topography with a camera: accuracy and geoscience application." *Journal of*
 492 *Geophysical Research: Earth Surface* 117: F03017. doi:
 493 10.1029/2011JF002289.

494 James, M. R., and S. Robson. 2014. "Mitigating systematic error in topographic models
 495 derived from UAV and ground-based image networks." *Earth Surface Processes*
 496 *and Landforms* 39: 1413-1420. doi: 10.1002/esp.3609.

497 Jaud, M., Letortu, P., Augereau, E., Le Dantec, N., Beauverger, M., Cuq, V., Prunier,
 498 C., Le Bivic, R., and C. Delacourt. 2017a. "Adequacy of pseudo-direct
 499 georeferencing of terrestrial laser scanning data for coastal landscape surveying
 500 against indirect georeferencing." *European Journal of Remote Sensing* 50 (1):
 501 155-165.

502 Jaud, M., Passot, S., Allemand, P., Le Dantec, N., Grandjean, P., Ammann, J., and C.
 503 Delacourt. 2017b. "Stratégies d'optimisation d'acquisition par drone pour
 504 limiter les distorsions lors de la reconstruction 3D par les logiciels Photoscan et
 505 MicMac." Poster presented at Journées CRITEX, Grenoble, May 10-12.

506 Javernick, L., Brasington, J., and B. Caruso. 2014. "Modelling the topography of
 507 shallow braided rivers using Structure-from-Motion photogrammetry."
 508 *Geomorphology* 213: 166-182. doi:10.1016/j.geomorph.2014.01.006.

509 Kaiser, A., Neugirg, F., Rock, G., Müller, C., Haas, F., Ries, J., and J. Schmidt. 2014.
 510 "Small-scale surface reconstruction and volume calculation of soil erosion in
 511 complex Moroccan gully morphology using structure from motion." *Remote*
 512 *Sensing* 6: 7050-7080.

513 Kromer, R. A., Abellán, A., Hutchinson, D. J., Lato, M., Edwards, T., and M.
 514 Jaboyedoff. 2015. "A 4D filtering and calibration technique for small-scale point
 515 cloud change detection with a terrestrial laser scanner." *Remote Sensing* 7:
 516 13029-13052.

517 Lague, D., Brodu, N. and J. Leroux. 2013. "Accurate 3D comparison of complex
518 topography with terrestrial laser scanner: Application to the Rangitikei canyon
519 (N-Z)." *ISPRS Journal of Photogrammetry Remote Sensing* 82: 10-26.

520 Laignel, B. 1997. "Les altérites à silex de l'ouest du Bassin de Paris: caractérisation
521 lithologique, genèse et utilisation potentielle comme granulats." PhD diss.,
522 University of Rouen.

523 Lato, M. J., Diederichs, M. S., and D. J. Hutchinson. 2010. "Bias Correction for View-
524 limited Lidar Scanning of Rock Outcrops for Structural Characterization." *Rock*
525 *Mechanics and Rock Engineering* 43: 615-628.

526 Laute, K., Letortu, P., Le Dantec, N. 2017. "Processes and mechanisms governing hard
527 rock cliff erosion in western Brittany, France." Poster presented at the EGU
528 General Assembly, Vienna, April 23-28.

529 Letortu, P., Costa, S., Bensaid, A., Cador, J. M., and H. Quénol. 2014. "Vitesses et
530 rythmes de recul des falaises crayeuses de Haute-Normandie (France) :
531 méthodologie et variabilité du recul." *Géomorphologie, relief, processus et*
532 *environnement* 2: 133-144.

533 Letortu, P., Costa, S., Cador, J. M., Coinaud, C., and O. Cantat. 2015a. "Statistical and
534 empirical analyses of the triggers of coastal chalk cliff failure." *Earth Surface*
535 *Processes and Landforms*, 40 (10): 1371-1386. doi: 10.1002/esp.3741

536 Letortu, P., Costa, S., Maquaire, O., Delacourt, C., Augereau, E., Davidson, R., Suanez,
537 S., and J. Nabucet. 2015b. "Retreat rates, modalities and agents responsible for
538 erosion along the coastal chalk cliffs of Upper Normandy: The contribution of
539 terrestrial laser scanning." *Geomorphology*, 245: 3-14. doi:
540 10.1016/j.geomorph.2015.05.007

541 Lichti, D., and J. Skaloud. 2010. "Registration and calibration." In *Airborne and*
542 *Terrestrial Laser Scanning*, edited by Vosselman G., and H. S. Maas, 83-133.
543 Whittles Publishing: Dunbeath.

544 Lim, M., Rosser, N. J., Petley, D. N., and M. Keen. 2011. "Quantifying the controls and
545 influence of tide and wave impacts on coastal rock cliff erosion." *Journal of*
546 *Coastal Research* 27: 46-56. doi:10.2112/JCOASTRES-D-09-00061.1

547 Medjkane, M., Maquaire, O., Costa, S., Roulland, T., Letortu, P., Fauchard, C., Antoine,
548 R., and R. Davidson. Accepted. "High resolution monitoring of complex coastal

549 morphology changes: Cross-efficiency of SfM and TLS based survey (Vaches-
550 Noires cliffs, Normandy, France).” *Landslides*.

551 Michoud, C., Carrea, D., Costa, S., Derron, M. H., Jaboyedoff, M., Davidson, R.,
552 Delacourt, C., Letortu, P., and O. Maquaire. 2014. “Landslide detection and
553 monitoring capability of boat-based mobile laser scanning along Dieppe coastal
554 cliffs, Normandy.” *Landslides*. doi: 10.1007/s10346-014-0542-5.

555 Mortimore, R. N., and A. Duperret. 2004. *Coastal chalk cliff instability*. Engineering
556 Geology Special Publications, London.

557 Naylor, L. A., Stephenson, W. J., and A. S. Trenhaile. 2010. “Rock coast
558 geomorphology: recent advances and future research directions.”
559 *Geomorphology* 114: 3-11.

560 Oppikofer, T., Jaboyedoff, M., Blikra, L., Derron, M. H., and R. Metzger. 2009.
561 “Characterization and monitoring of the Åknes rockslide using terrestrial laser
562 scanning.” *Natural Hazards Earth System Sciences* 9: 1003-1009.

563 Pesci, A., Teza, G., and E. Bonali. 2011. “Terrestrial laser scanner resolution: numerical
564 simulations and experiments on spatial sampling optimization.” *Remote Sensing*
565 3: 167-184.

566 Pirotti, F. 2013. “State of the art of ground and aerial laser scanning technologies for
567 high-resolution topography of the earth surface.” *EuJRS* 46: 66-78.

568 Pomerol, B., Bailey, H. W., Monciardini, C., and R. N. Mortimore. 1987.
569 “Lithostratigraphy and biostratigraphy of the Lewes and Seaford chalks: a link
570 across the Anglo-Paris basin at the Turonian-Senonian boundary.” *Cretaceous*
571 *Research* 8: 289-304

572 Raber, G. T., Jensen, J. R., Hodgson, M. E., Tullis, J. A., Davis, B. A., and J. Berglund.
573 2007. “Impact of Lidar nominal post-spacing on DEM accuracy and flood zone
574 delineation.” *Photogrammetry Engineering Remote Sensing* 73: 793-804.

575 Riegl. 2014. Data sheet VZ-400. 4p

576 Smith, M. W., Carrivick, J. L., Hooke, J., and M. J. Kirkby. 2014. “Reconstructing
577 Flash Flood Magnitudes Using ‘Structure-from-Motion’: a rapid assessment
578 tool.” *Journal of Hydrology* 519: 1914-1927.

579 Smith, M. W., Carrivick, J., and D. Quincey. 2016. “Structure from motion
580 photogrammetry in physical geography.” *Progress in physical geography* 40:
581 247-275

- Sturzenegger, M., and D. Stead. 2009. "Quantifying discontinuity orientation and persistence on high mountain rock slopes and large landslides using terrestrial remote sensing techniques." *Natural Hazards Earth System Sciences* 9: 267–287.
- Su, J., and E. Bork. 2006. "Influence of vegetation, slope, and lidar sampling angle on DEM accuracy." *Photogrammetry Engineering Remote Sensing* 72: 1265-1274.
- Teza, G., Galgaro, A., Zaltron, N., and R. Genevois. 2007. "Terrestrial laser scanner to detect landslide displacement fields: A new approach." *International Journal Remote Sensing* 28: 3425-3446.
- Vann Jones, E. C. (née Norman), Rosser, N. J., Brain, M. J., and D. N. Petley. 2015. "Quantifying the environmental controls on erosion of a hard rock cliff." *Marine Geology* 363: 230-242.
- Westoby, M., Brasington, J., Glasser, N., Hambrey, M., and J. Reynolds. 2012. "'Structure-from-Motion" photogrammetry: A low cost, effective tool for geoscience applications." *Geomorphology* 179: 300-314.
- Young, A. P., Olsen, M. J., Driscoll, N., Rick, R. E., Gutierrez, R., Guza, R. T., Johnstone, E., and F. Kuester. 2010. "Comparison of airborne and terrestrial lidar estimates of seacliff erosion in Southern California." *Photogrammetric Engineering & Remote Sensing* 76: 421–427.
- Young, A. P. 2015. "Recent deep-seated coastal landsliding at San Onofre State Beach, California." *Geomorphology* 228: 200–212.

Tables

Method	Number of points	Surface (m ²)	Average density per m ² on the cliff face	Sampling distance on cliff face for the raw point cloud
Terrestrial photogrammetry (TP)	124,757, 214	13,897	8,977	Irregular: mean of 1 point every 0.0105 m
UAV photogrammetry (UAVP)	59,418,289	15,535	3,824	Regular: mean of 1 point every 0.016 (mean)

Terrestrial laser scanning (TLS)	2,553,230	14,190	178	Irregular: mean of 1 point every 0.06 m (mean)
---	-----------	--------	-----	--

605 Table 1. Main characteristics of raw datasets

		TLS	TP_SF	UAVP_SF
Main characteristics	Number of points	2,264,742	2,030,389	2,160,790
	Mean density (per m²)	293 (± 159)	183 (± 17)	171 (± 15)
	Density interval per m²	1-657	1-355	1-396
Advantages		Few occlusions (except caves where the TLS station is not well positioned)	Homogeneous density (less than UAVP because manual snapping is more irregular)	Homogeneous density and there are no occlusions at cliff top and cliff foot
Disadvantages		Heterogeneous density due to TLS stations and there are some occlusions due to rock fall and hollow terrain	Occlusions (overhanging areas at cliff top, rock fall at cliff foot)	

606 Table 2. Characteristics, advantages and disadvantages of the TLS, TP and UAVP point
607 clouds (after subsampling and cleaning)

	TP point cloud vs. TLS mesh		UAVP point cloud vs. TLS mesh	
	Mean error	Standard deviation	Mean error	Standard deviation
Whole cliff face	0.005	0.05	0.014	0.037

608 Table 3. Mean error and standard deviation values (m) between TP and UAVP whole
609 cliff-face point clouds vs. TLS mesh

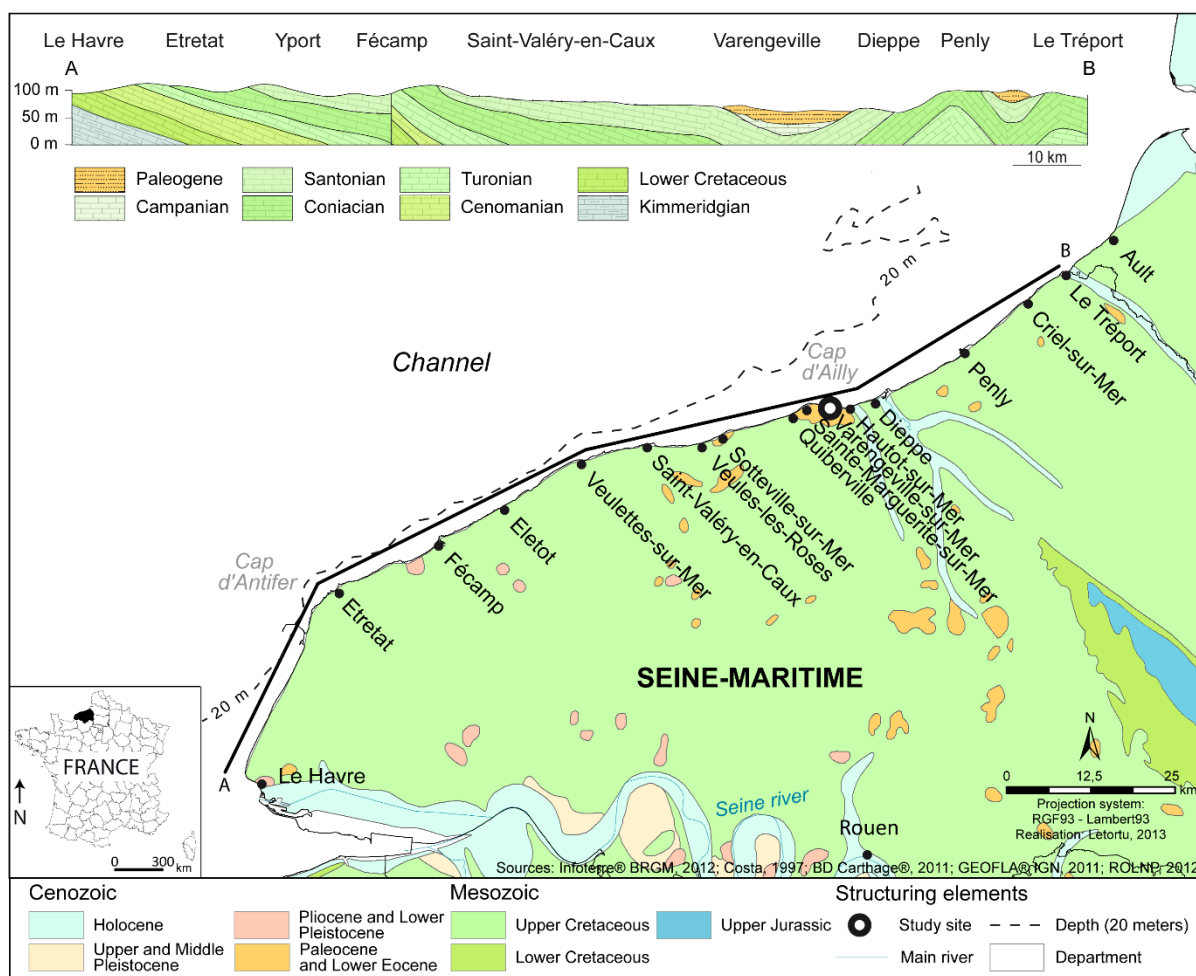
	TLS (Riegl® VZ-400 or similar)	TP (Nikon D800 or similar)	UAVP (DS6 + Nikon D800 or similar)
--	---	---	---

Precision	high	low	high
Purchase and maintenance costs	very expensive (purchase: 150 k€)	cheap (purchase: 1.5 k€)	expensive (purchase: 10 k€)
Weight (instruments and targets)	very heavy (33 kg)	light (5 kg)	heavy (9 kg)
Battery life	long	very long	short
Speed of data acquisition	low	low	very high
Sensitivity to occlusion	high	high	very low
Sensitivity to bad weather (rainfall, wind)	high	very low	high
Number of man/days	high	low	high
Ability to implement survey (targets, pilot, station location)	poor	very good	good
Flexibility in the ability to capture the interest area (overhanging, caves, etc.)	low	low	very high
Level of acquisition skill needed	high	high	very high
Acquisition duration	long	long	short
Processing duration	long	very long	very long

610 Table 4. Summary of strengths (significant strengths in green in the online version, light
611 gray in the print version) and weaknesses (significant weaknesses in red in the online
612 version, dark gray in the print version) of TLS, TP and UAVP methods for Normandy
613 cliff erosion monitoring

614

615 **List of figures**



616

617 Figure 1. Presentation of the study area

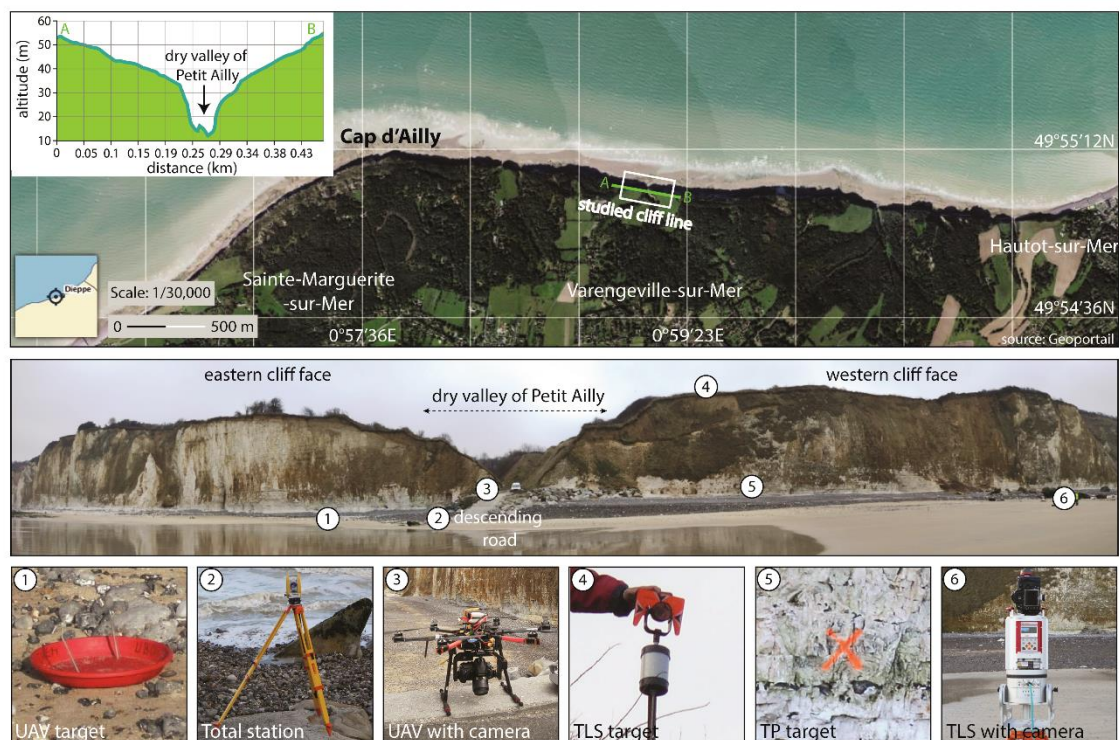


Figure 2. Panorama of Petit Ailly cliff face (Varengueville-sur-Mer) and instrumentation used for the survey (28 January 2016)

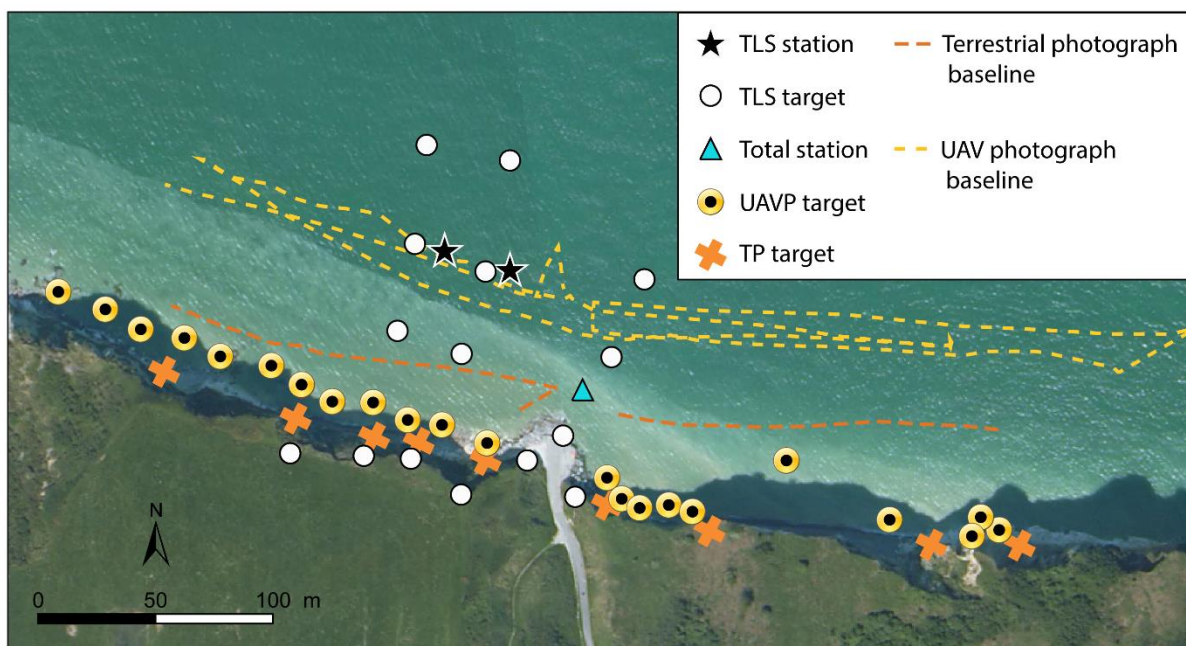


Figure 3. Location of the instruments, GCPs and protocol for the survey (28 January 2016) (cliff-top view)

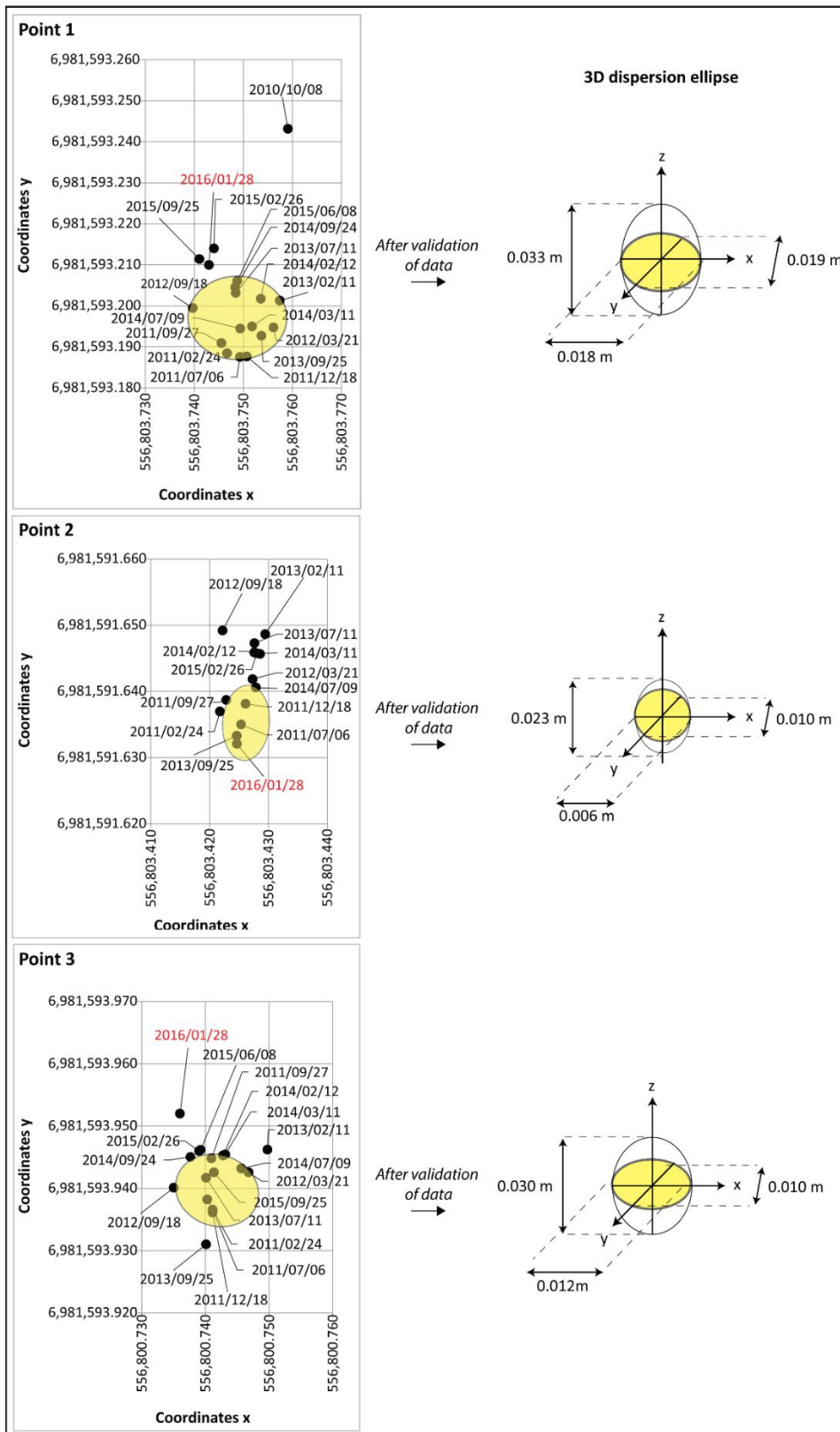
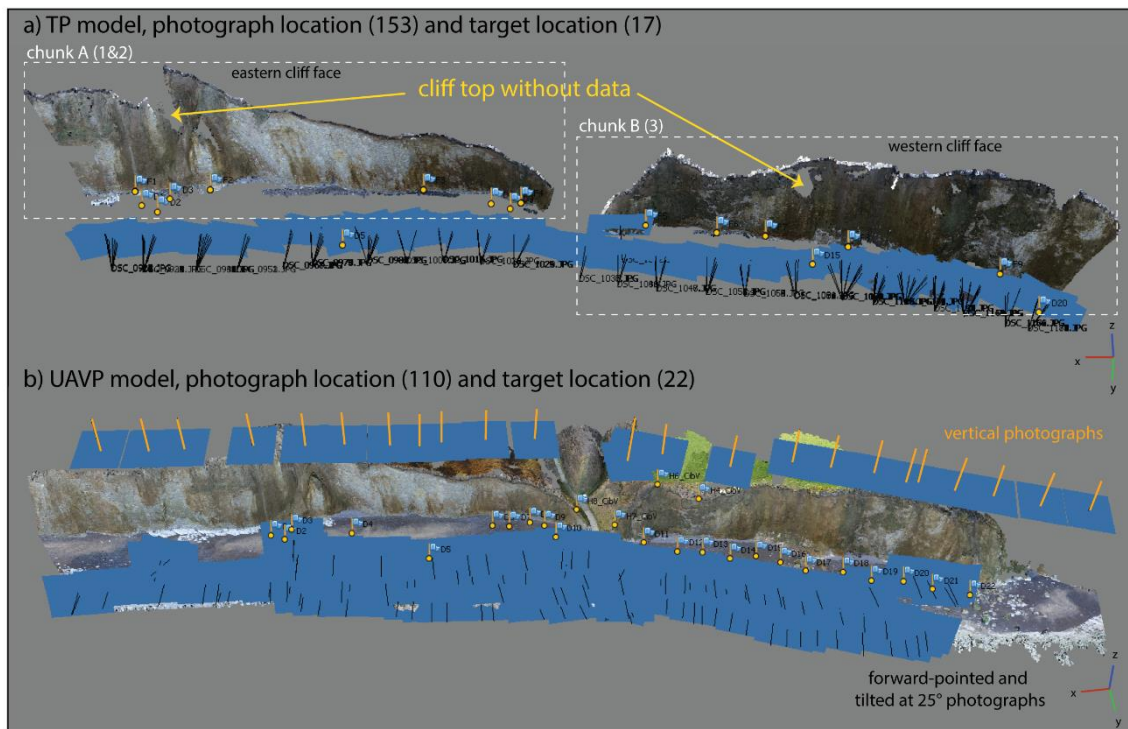


Figure 4. Maximum dispersion ellipses measured by the total station at surveyor nails for the long-term monitoring (the survey used in this paper is depicted in orange in the online edition)



629

630 Figure 5. Location and overlap of photographs, location of GCPs, and TP and UAVP
 631 models

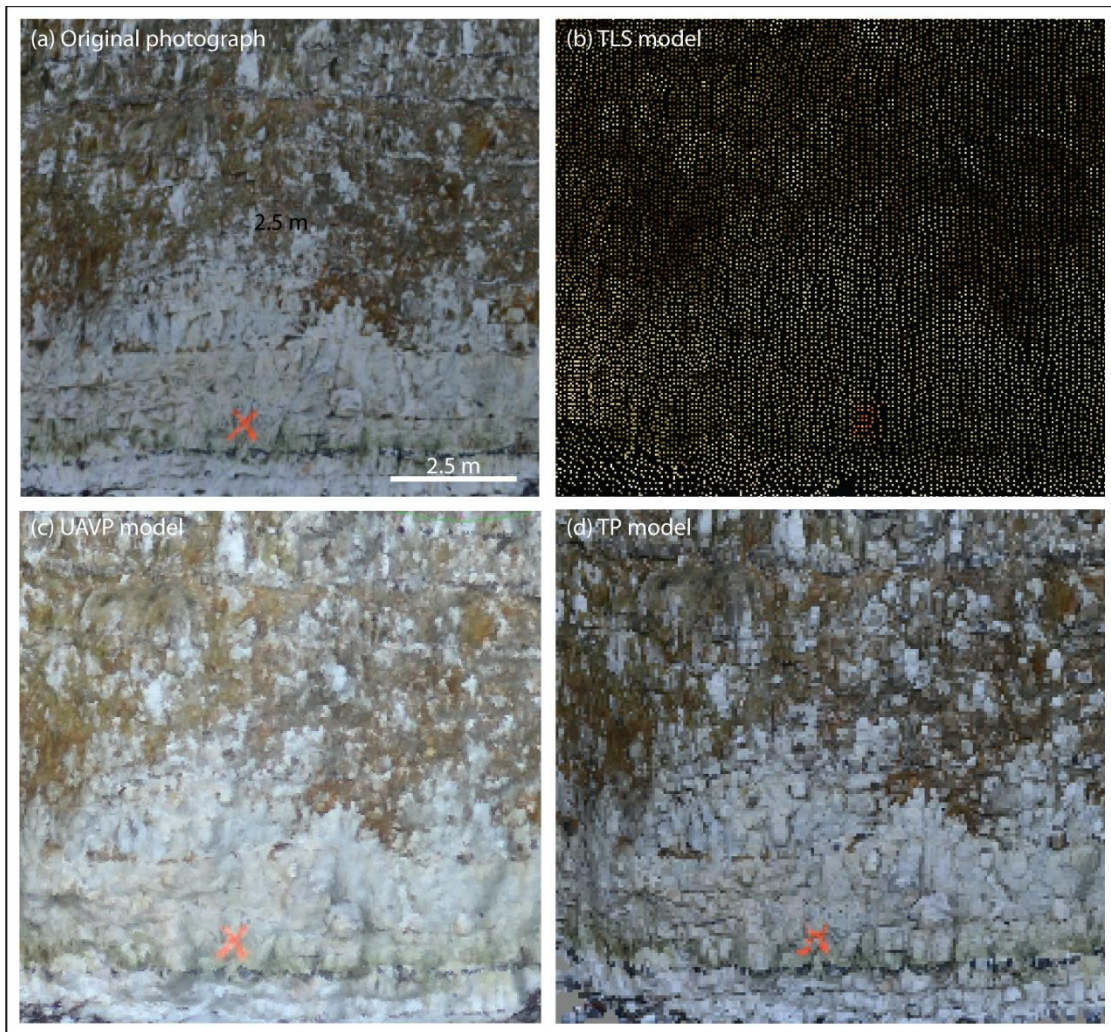


Figure 6. Cliff face zoom from (a) original photograph, (b) TLS model, (c) UAVP model and (d) TP model

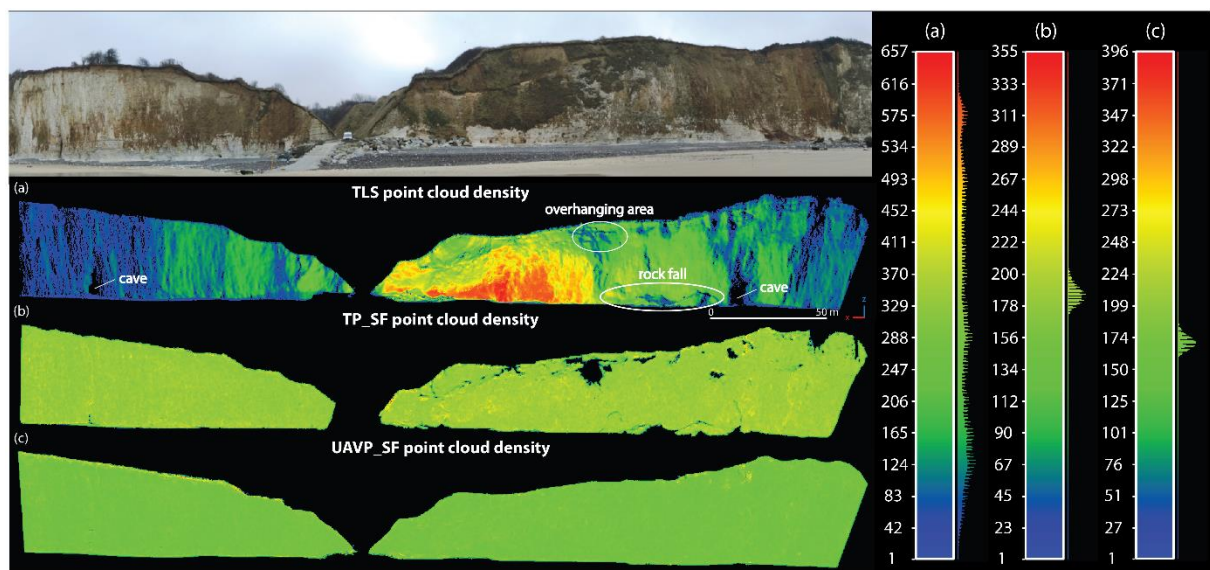


Figure 7. Density of point clouds per m² (TLS, TP, UAVP)

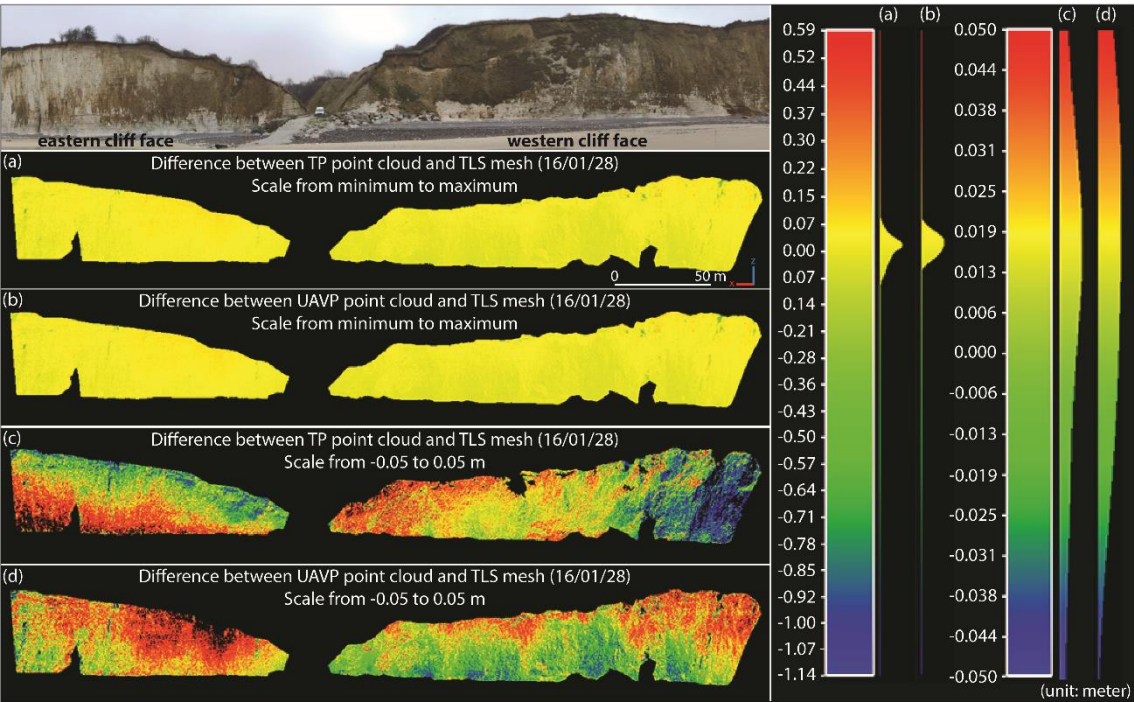


Figure 8. Distribution of difference between datasets over the cliff face

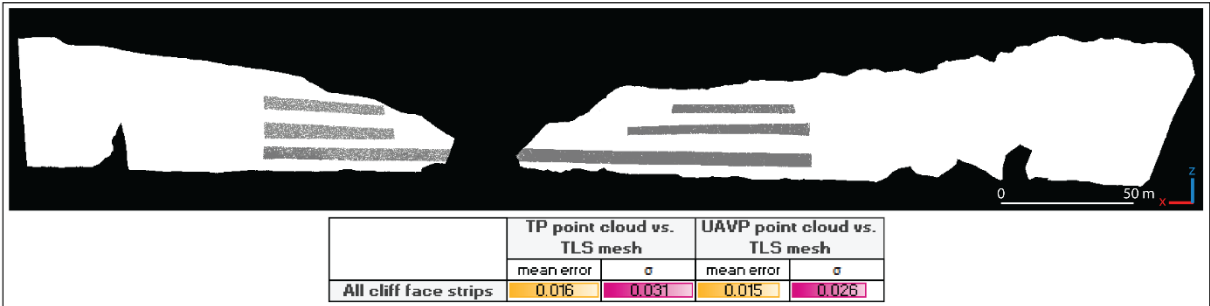


Figure 9. Comparison between all cliff-face strip error values and standard deviation

643 Acknowledgements

644 This work is part of the Service National d'Observation DYNALIT, via the research
645 infrastructure ILICO. The authors thank the reviewers for their helpful comments to improve
646 the quality of the manuscript.

647

648 Funding

649 This work was supported by the French “Agence Nationale de la Recherche” through the
650 “Laboratoire d'Excellence” LabexMER [ANR-10-LABX-19-01] program, and co-funded by a
651 grant from the French government through the “Investissements d'Avenir” and the Brittany
652 Region. This work was also supported by the ANR project “RICOCHET: multi-risk assessment
653 on coastal territory in a global change context” funded by the French Research National Agency
654 [ANR-16-CE03-0008]. Finally, this work was supported by the CNES (the French space
655 agency) thanks to TOSCA project EROFALITT.